Biochemistry

 Volume 32, Number 37 September 21, 1993

Articles

Lipid Effects on Aggregation of Pulmonary Surfactant Protein SP-C Studied by Fluorescence Energy Transfer†

Ann D. Horowitz,* John E. Baatz,‡ and Jeffrey A. Whitsett

Division of Pulmonary Biology, Children's Hospital Medical Center, Children's Hospital Research Foundation, Elland and Bethesda Avenues, Cincinnati, Ohio 45229

Received December 9, 1992; Revised Manuscript Received June 28, 1993®

ABSTRACT: The self-association of pulmonary surfactant protein SP-C in lipid vesicles was studied using fluorescence energy transfer. Bovine SP-C was labeled with two fluorescent probes, succinimidyl 6-[*N*-(7-nitrobenz-2-oxa-1,3-diazol-4-yl)amino]hexanoate and eosin isothiocyanate, on the amino terminus of the protein, producing NBD-SP-C and EITC-SP-C, respectively. The N-terminus of SP-C was relatively immobile between 20 and 37 °C, as demonstrated by high fluorescence anisotropy of NBD-SP-C and EITC-SP-C. The mobility increased at the transition of the lipid to the fluid phase. Using fluorescence energy transer, with NBD-SP-C as the donor and EITC-SP-C as the acceptor, a high degree of SP-C/SP-C association was found below 25 °C, decreasing to very little self-association above 42 °C in 7:1 1,2-dipalmitoylphosphatidylcholine–1,2-dipalmitoylphosphatidylglycerol (DPPC–DPPG) vesicles. The fraction of SP-C aggregated below 37 °C in 7:1 DPPC–DPPG was estimated from the observed energy transfer to be more than 70% of total SP-C. In various lipid mixtures, self-association of SP-C was dependent on the presence of at least some gel-phase lipids. In a lipid mixture resembling pulmonary surfactant, gradually increasing self-association was observed below 38 °C. The relation of the present data to the state of aggregation of SP-C in pulmonary surfactant is discussed.

Pulmonary surfactant is a lipid–protein complex secreted by type II epithelial cells lining the alveoli of the lung. The lipid–protein complex forms a film at the air–liquid interface and prevents collapse of the distal components of the lung by dramatically lowering surface tension within the alveolus (Goerke, 1974; Harwood & Richards, 1985). Respiratory distress syndrome (RDS), a major cause of neonatal morbidity and mortality arising from a deficit in pulmonary surfactant in the lungs of premature infants, can be treated through surfactant replacement. Organic extracts of surfactant are enriched in saturated phospholipids, such as dipalmitoylphosphatidylcholine (DPPC), and contain two small hydrophobic proteins which greatly enhance the effectiveness of the lipid components both *in vivo* and *in vitro* (Whitsett et al., 1986; Yu & Possmayer, 1986; Hawgood et al., 1987; Curstedt et al., 1987).

The surfactant-associated proteins, SP-B and SP-C, contain predominantly hydrophobic domains. Bovine SP-C contains 34 amino acid residues of which 23 are valine, leucine, or isoleucine (Whitsett et al., 1986; Wilkinson et al., 1987; Johansson et al., 1988). In addition, two palmitic acid residues are attached via thio ester linkages to the adjacent cysteines in the N-terminal region of SP-C (Curstedt et al., 1990). The central and C-terminal regions of the peptide (residues 12–34) contain exclusively nonpolar amino acids. Both SP-B and SP-C lower surface tension and increase the rate of adsorption of lipid monolayers to the air–water interface (Notter et al., 1983, 1987; Curstedt et al., 1987). SP-C

† This work was supported by NIH Training Grant HL07527 (A.D.H.) and by an American Lung Association research grant (A.D.H.).

* To whom correspondence should be addressed.

‡ Current address: Department of Pediatrics, Division of Neonatology, Medical University of South Carolina, 171 Ashley Ave., Charleston, SC 29425.

® Abstract published in *Advance ACS Abstracts*, September 1, 1993.

0006-2960/93/0432-9513$04.00/0

contains a high proportion of α-helix (Whitsett & Baatz, 1992; Vandenbussche et al., 1992; Pastrana et al., 1991), which is predicted by primary structural analysis to lie in the region of residues 10–34, providing a very hydrophobic helical region of sufficient length to span a lipid bilayer (Whitsett & Baatz, 1992; Pastrana et al., 1991).

In lipid vesicles at a 1:500 protein:lipid molar ratio, SP-C lowers the phase transition temperature, T_m, of DMPC or DPPC–DPPG[1] mixtures and broadens the phase transition (Horowitz et al., 1992; Simatos et al., 1990). At higher concentrations, SP-C causes an increase in vesicle size (Rice et al., 1989). Mixtures of SP-C and SP-B also cause leakiness and fusion of vesicles (Shiffer et al., 1988).

When purified SP-C or surfactant protein mixtures containing SP-C are subjected to SDS–PAGE, some SP-C is frequently observed to migrate as a dimer, which can be reduced to a monomer by thiols. An SP-C dimer had recently been identified which has a secondary structure markedly different from the SP-C monomer (Baatz et al., 1992). The aggregation state of native SP-C in surfactant is not known.

Fluorescence resonance energy transfer (ET) has found numerous applications in membrane systems for determining the association and proximity of proteins in membranes and monitoring lipid-phase separations and fusion of lipid vesicles. In the present work, ET is used to determine whether monomers of SP-C interact directly in a lipid environment. Distinct samples of SP-C were labeled with the fluorescent probes succinimidyl NBD-hexanoate and eosin isothiocyanate (EITC). The degree of self-association of labeled SP-C molecules in multilamellar lipid vesicles was monitored by quenching of donor fluorescence in the presence of acceptor, using NBD-SP-C as a donor and EITC-SP-C as an acceptor. Multilamellar vesicles were used because they more closely resemble the multilamellar structures present in native surfactant and in lamellar bodies of pulmonary type II cells.

EXPERIMENTAL PROCEDURES

Materials. Methanol and chloroform were Optima grade from Fisher Scientific, Cincinnati, OH. All lipids were from Avanti Polar Lipids, Alabaster, AL, except for DMPC and DSPC, which were from Sigma Chemical Co., St. Louis, MO. Succinimidyl NBD-hexanoate and eosin isothiocyanate were from Molecular Probes, Inc., Eugene, OR. Silicic acid column chromatography material was Bio-Sil HA minus 325 mesh from Bio-Rad Co., Richmond, CA. Lipophilic Sephadex LH-60 was obtained from Sigma Chemical Co.

Purification of SP-C. SP-C was isolated from cow lungs by methods described previously (Whitsett et al., 1986). Briefly, freshly excised lungs were lavaged with 0.15 N saline, and surfactant was pelleted by centrifugation. Surfactant was extracted with $CHCl_3/CH_3OH$ (C/M), and the extract was dialyzed against the same solvent. SP-C was purified from the dialysate by passage through a silicic acid column using a stepwise gradient of C/M. The fractions containing SP-C were identified by SDS–PAGE. SP-C was further purified by chromatography on lipophilic Sephadex LH-60 in 1:1 C/M containing 0.001 M HCl. Prolonged dialysis against the latter solvent was utilized to remove contaminating lipids. Column chromatography and dialysis were repeated until a sufficiently pure preparation of SP-C was obtained. In the final dialysis step, the purified SP-C was dialyzed against 2:1 C/M to remove the HCl. SP-C was stored as a C/M (2:1 v/v) solution. Purity of SP-C was determined by SDS–PAGE (Laemmli, 1970) on 17% acrylamide gels, and SP-C concentration was determined by amino acid compositional analysis (Ross et al., 1986). SP-C generated by this methodology contained no detectable SP-B as assessed by Western blot analysis using SP-B-specific antisera.

Fluorescent Labeling of SP-C. SP-C in 2:1 C/M was mixed with a 4-fold molar excess of NBD-succinimide in 2:1 C/M which had been adjusted to pH 7.6 with 0.2 M HEPES. The reaction was allowed to proceed in an amber reaction vial with stirring at room temperature overnight. A 25-μL aliquot of 1 M Tris-HCl was added to deplete excess reactant, and the mixture was dialyzed against 1:1 C/M. The labeled SP-C was separated from free NBD by chromatography on lipophilic Sephadex LH-60 in 1:1 C/M and 0.01 M HCl, followed by dialysis against 1:1 C/M, and chromatography on silica gel in stepwise mixtures of C/M from 20:1 (v/v) to 0:1. The fractions containing NBD-labeled SP-C were identified by gel electrophoresis (Laemmli, 1970), followed by examination under UV illumination. Reaction of SP-C with EITC was carried out in a similar manner, except that the molar excess of EITC used was 45-fold, and the reaction lasted 3 h at room temperature. Purification was obtained by chromatography on LH-60 and subsequent dialysis. Labeling efficiencies were calculated using an extinction coefficient of 1.7×10^3 at 466 nm for NBD succinimide and 101×10^3 for EITC. Protein concentrations were determined by amino acid compositional analysis. Water-soluble amino acid analogues of EITC-SP-C and NBD-SP-C were made by reacting an excess of leucine with EITC or succinimidyl NBD-hexanoate under similar conditions.

To determine whether the fluorescent label was located at the amino terminus of the SP-C molecule, 1.1 nmol of each sample was subjected to gas-phase N-terminal sequence analysis on a Porton 2090E protein sequencer in the protein chemistry facility in the Department of Pharmacology and Cell Biophysics of the University of Cincinnati.

Surface Activity Measurements. The surface activity of protein–lipid mixtures was assessed using a Wilhelmy surface balance-langmuir trough as described previously (Baatz et al., 1992; Baatz et al., 1991). The lipid mixture, 68:22:9 DPPC–egg PG–palmitic acid (w/w/w), was mixed with the SP-C sample being tested in C/M solution to give a protein:lipid ratio of 2% (w/w). Solvent was removed by rotary evaporation by the procedure described previously (Baatz et al., 1992), and samples were then suspended in 1 mL of 150 mM NaCl. All samples were incubated for at least 24 h at 4 °C prior to testing.

Fourier Transform Infrared Spectroscopy. Fourier transform infrared spectroscopy (FTIR) was carried out on a Bio-Rad Digilab FTS-40 spectrometer at room temperature with a DGTS detector. SP-C samples mixed with 7:1 DPPC–DPPG at a 3% w/w protein:lipid ratio in C/M solution were layered onto the germanium ATR (attenuated total reflection) crystal to form an iridescent film upon sample evaporation. For each spectrum 256 interferograms of sample and background were collected at 2-cm^{-1} resolution and signal-averaged.

[1] Abbreviations: NBD, 7-nitrobenz-2-oxa-1,3-diazole; EITC, eosin isothiocyanate; MOPS, 3-(*N*-morpholino)propanesulfonic acid; HEPES, *N*-(2-hydroxyethyl)piperazine-*N*'-2-ethanesulfonic acid; MNE, 10 mM MOPS, 120 mM NaCl, and 2 mM EDTA buffer, pH 7.0; ET, energy transfer; FTIR, Fourier transform infrared spectroscopy; DPPC, 1,2-dipalmitoyl-*sn*-glycero-3-phosphocholine; DPPG, 1,2-dipalmitoyl-*sn*-glycero-3-phospho-*sn*-glycerol; NBD-PC, 1-palmitoyl-2-[6-[*N*-(7-nitrobenz-2-oxa-1,3-diazol-4-yl)amino]caproyl]-*sn*-glycero-3-phosphocholine; POPC, 1-palmitoyl-2-oleoyl-*sn*-glycero-3-phosphocholine; POPG, 1-palmitoyl-2-oleoyl-*sn*-glycero-3-phospho-*sn*-glycerol; DMPC, 1,2-dimyristoyl-*sn*-glycero-3-phosphocholine; DSPC, 1,2-distearoyl-*sn*-glycero-3-phosphocholine; C/M, chloroform/methanol solution.

The interferograms were apodized with a triangular function and Fourier transformed. An additional spectra was obtained of lipid alone. This was subtracted from each of the SP-C–lipid spectra prior to analysis. The resultant spectra were deconvoluted with a half-width of 15 and $k = 2.1$ to obtain the peak centers of the component peaks. Spectral fitting (Peakfit software, Jandel Scientific) was carried out using Gaussian spectral components, with the peak centers held constant at the values determined by deconvolution, while peak widths and heights were variable. For all curve fits, r^2 was 0.995 or higher. The percent α-helix was calculated as the percent of the total amide I peak area contributed by the component centered at 1655–1656 cm^{-1}. The EITC-SP-C sample used for FTIR was the sample with 32% labeling efficiency.

Preparation of Multilamellar Vesicles. Stock solutions of phospholipids in chloroform were mixed with SP-C in 2:1 C/M solution to give the protein:lipid ratio desired. The protein–lipid mixtures were incubated at 50 °C while being dried under a gentle stream of nitrogen. Two milliliters of buffer consisting of 10 mM MOPS, 120 mM NaCl, and 2 mM EDTA, pH 7.0 (MNE buffer) at 50 °C, was added the dried film, followed by incubation for 30 min at 50 °C. Multilamellar vesicles were formed upon vortexing for 30 s as described previously (Horowitz et al., 1992; Baatz et al., 1990) and sonicated for 30 s in an EM/C bath ultrasonicator at room temperature in order to reduce aggregation of vesicles. Vesicles were allowed to air cool to room temperature and then equilibrated at 20 °C for 30 min prior to beginning the experiment. With each temperature change, at least 10 min was allowed for equilibration at the new temperature. For collisional quenching experiments, multilamellar dispersions were sonicated at 60 W for 1 min at 0 °C using a Cole-Parmer 4710 series sonicator equipped with a microtip.

Column chromatography of lipid vesicles containing SP-C was conducted on a 1.5 × 15 cm Sepharose 6B column in MNE buffer at room temperature.

Energy Transfer and Fluorescence Measurements. Fluorescence measurements were conducted using a Perkin-Elmer LS-50 fluorometer. The temperature in the sample chamber was controlled (±0.5 °C) using a Lauda circulating water bath. The samples were allowed to equilibrate at the initial temperature for at least 30 min, with gentle stirring. The temperature was increased gradually over the course of the experiment from 20 to 50 °C. For each energy transfer experiment, four samples were used (Fairclough & Cantor, 1978): B, a background sample in which none of the components were fluorescently labeled; D, a sample containing donor-labeled SP-C (NBD-SP-C); A, a sample containing acceptor-labeled SP-C (EITC-SP-C); and DA, a sample containing both donor- and acceptor-labeled SP-C. In all samples the total SP-C concentration was maintained constant by inclusion of the appropriate amount of unlabeled SP-C. Excitation was at 460 nm, and donor fluorescence was measured at three wavelengths at which the contribution of the acceptor was minimal, 510, 515, and 520 nm. At the end of the experiment, the vesicles were disrupted by addition of sufficient 10% Triton X-100 to bring the final concentration to 1% Triton X-100, with the temperature maintained at 48–50 °C. This treatment was performed to abolish the energy transfer. Energy transfer (ET) was calculated from the raw data as follows: first, the contribution of the background light scattering was subtracted from all data. Possible differences in donor concentration between the D and DA samples were corrected using the donor fluorescence observed in 1% Triton X-100 at 50 °C (Wolf et al., 1992). The ET efficiency E was then calculated at each wavelength according to

$$E = 1 - \frac{Q_{DA}}{Q_D} = 1 - \frac{(F_{DA} - F_A)}{F_D} \quad (1)$$

where F_D, F_{DA}, and F_A are the fluorescence of the D, DA, and A samples. The ET calculated at the three wavelengths was averaged.

R_o is the distance at which the energy transfer efficiency of an isolated donor/acceptor pair is 50%. For each donor/acceptor pair, R_o was calculated from the spectral characteristics of the fluorophores [see, for example, Cantor and Schimmel (1980)], using the value of 1.33 for the refractive index of water (Weast, 1973). The dipole–dipole orientation factor, κ^2, was assumed to be $^2/_3$, which corresponds to the case in which donor and acceptor are free to tumble rapidly on the time scale of fluorescence (the lifetime of the donor, approximately 9 ns). At some temperatures examined in these experiments, both donor and acceptor have a high fluorescence anisotropy, indicating that the assumption of $\kappa^2 = {}^2/_3$ is not correct. For the case of a random distribution of donors and acceptors in the bilayer, the effect of measuring ET over a distribution of rigid donor and acceptor orientations enters as a scaling factor in the concentration of acceptor (Wolber & Hudson, 1979). Although the effect is not explicitly treated in our approach, it is likely to be small, based on the anisotropies of the donor and acceptor, even at low temperatures where they are most rigidly held.[2]

Corrected emission spectra for quantum yields and calculation of the overlap integral were obtained using quinine sulfate in 0.1 N H_2SO_4 as a standard (White & Argauer, 1970). The quantum yield of NBD-SP-C and EITC-SP-C in 1% Triton X-100 at 20 °C was measured relative to sodium fluorescein in 0.1 N NaOH, using a quantum yield of 0.92 for the fluorescein (Weber & Teale, 1957). The quantum yields of NBD-SP-C and EITC-SP-C in lipid vesicles at various temperatures were then obtained relative to the respective quantum yield in 1% Triton X-100 at 20 °C.

The fluorescence anisotropy of NBD-SP-C was measured with excitation at 460 nm and emission at 520 nm. For EITC-SP-C the excitation was at 520 nm and emission at 547 nm. The intensities of the parallel and perpendicular components of the emitted light were corrected for scattered light by subtracting the corresponding intensities of the background sample (Gelborn & Sawyer, 1978).

RESULTS

SP-C labeled with NBD-succinimide or EITC migrated as a single band on SDS–PAGE, at the same mobility as unlabeled SP-C (Figure 1). The extent of labeling as determined from the absorbance of the fluorophores was 105% for NBD-SP-C and 64.5% for EITC-SP-C. A second sample of EITC-SP-C was also obtained, with a labeling efficiency of 32%. The EITC-SP-C sample with the higher labeling efficiency was used for the experiments described herein, unless otherwise stated. When used at the same final EITC concentration, the two EITC-SP-C samples gave identical results. Protein sequence analysis of EITC-SP-C by Edman degradation

[2] In dual-labeled polymers, the effect of measuring ET over a distribution of random but rigid donor and acceptor orientations is small even for anisotropies as high as 0.31 (Haas et al., 1978); however, those experiments were not conduced in a system undergoing a lipid-phase transition. In the case of the formation of specific dimers or oligomers of SP-C, the deviation of κ^2 from $^2/_3$ would be significant if we were to attempt to determine the ET efficiency within the oligomer.

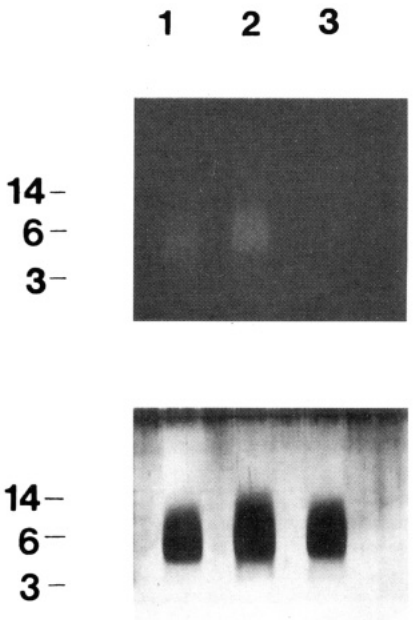

FIGURE 1: SDS–PAGE of NBD-SP-C and EITC-SP-C. Fluorescence of the labeled protein is viewed under ultraviolet illumination at 300 nm using a red filter. Lanes: 1, NBD-SP-C; 2, EITC-SP-C; 3, native SP-C. M_r values ($\times 10^{-3}$) of standards are indicated on the left.

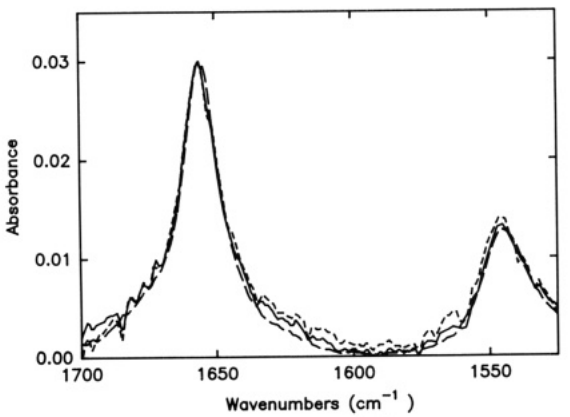

FIGURE 2: Amide I and II region of Fourier transform infrared spectra of SP-C samples at a 3% (w/w) protein/lipid ratio in 7:1 DPPC–DPPG film on a Ge ATR crystal. The spectrum of a 7:1 DPPC–DPPG film was subtracted from each sample spectrum. Spectra shown have been zeroed and scaled. SP-C samples are (solid) SP-C, (long dash) NBD-SP-C, and (short dash) EITC-SP-C.

resulted in only a 14% yield. In the case of NBD-SP-C, the amino terminus was completely blocked, resulting in no detectable degradation. The resistance of Edman degradation acquired by the labeled SP-C demonstrates that the samples are both labeled on the amino terminus of the protein.

Fourier transform infrared (FTIR) spectra of NBD-SP-C and EITC-SP-C were compared with that of native SP-C to determine the degree to which labeling may have altered the secondary structure of SP-C. The FTIR spectra of the three samples in the amide I and amide II regions are very similar (Figure 2). The amide I band, appearing between 1700 and 1600 cm^{-1}, contains component peaks which are identified with the secondary structures of the protein sample. SP-C samples are characterized by a narrow amide I peak, which has been reported to contain from 40% to 90% α-helical components (Vandenbussche et al., 1992; Pastrana et al., 1991; Baatz et al., 1992). In the native SP-C sample, a narrow peak accounting for 68% of the amide I band was found centered at 1656 cm^{-1}, a peak position consistent with α-helical structure

Table I: Summary of FTIR Data

peak location (cm^{-1})	width at half-max (cm^{-1})	% of total area	structural assignment
	SP-C		
1621.4	14.3	5.3	β-sheet
1631.5	6.7	2.8	β-sheet
1640.7	10.8	10.3	random
1656.1	15.4	67.5	α-helix
1672.5	10.4	9.4	β-turn
1680.4	5.8	2.4	β-turn
1689.6	8.6	2.3	β-sheet or turn
	EITC-SP-C		
1621.0	22.6	7.8	β-sheet
1640.8	19.1	16.7	random
1656.6	16.0	58.7	α-helix
1673.0	10.9	9.8	β-turn
1680.7	6.3	3.1	β-turn
1689.8	10.2	4.0	β-sheet or turn
	NBD-SP-C		
1628.5	22.9	8.7	β-sheet
1641.2	11.8	8.3	random
1655.5	14.8	61.6	α-helix
1670.7	12.0	11.4	β-turn
1680.8	11.8	5.3	β-turn
1690.6	18.4	4.6	β-sheet or turn

(Table I). The area assigned to random structure contributed 10% of the amide I area, while the total assigned to β-sheet and turns was 22%. The proportion of α-helix observed for NBD-SP-C was 62%. The amount of random structure observed in NBD-SP-C decreased slightly with labeling (to 8%), accompanied by a small increase in the total area attributed to β-sheet and turn structures (to 30%). In the case of EITC-SP-C the proportion of α-helix observed was 59%. Random structure increased relative to unlabeled SP-C (to 17%), while the proportion of the total area attributed to β-sheet and turns increased very slightly (to 25%).

The retention of biophysical activity by the labeled SP-C's was assessed by measuring the ability of fluorescently labeled SP-C to decrease surface tension of a lipid film at the air–water interface in a Wilhelmy surface balance apparatus (Baatz et al., 1991). NBD-SP-C was almost as active at lowering the minimum surface tension as was native SP-C (2.5 mN as compared with 0.3 mN). The equilibrium and maximum values for SP-C were 35 and 62 mN and for NBD-SP-C were 31.5 and 57 mN, respectively. Lipid alone displayed minimum, equilibrium, and maximum surface tension values of 16, 60, and 61 mN, respectively. The surface activity observed with EITC-SP-C was intermediate, with a minimum surface tension of 9.5 mN. Equilibrium and maximum surface tension values for EITC-SP-C were 46 and 61 mN.

Multilamellar vesicles were prepared from 7:1 DPPC–DPPG and native SP-C or NBD-SP-C or EITC-SP-C. Vesicles were separated from any unincorporated material by column chromatography on Sepharose 6B in MNE buffer at room temperature. Vesicular material eluted in the void volume, as monitored by light scattering at 360 nm. Lipid vesicles containing fluorescently labeled SP-C eluted at the same volume, as monitored by fluorescence at 520 nm (NBD-SP-C) or 547 nm (EITC-SP-C) (Figure 3). The column profiles demonstrated that the labeled SP-C molecules associate strongly with lipids, similarly to native SP-C. Since virtually all the fluorescence was associated with the vesicles, column purification of vesicles was omitted in subsequent experiments.

Fluorescence of Labeled SP-C. The fluorescence of NBD is highly dependent on the polarity of the medium. The

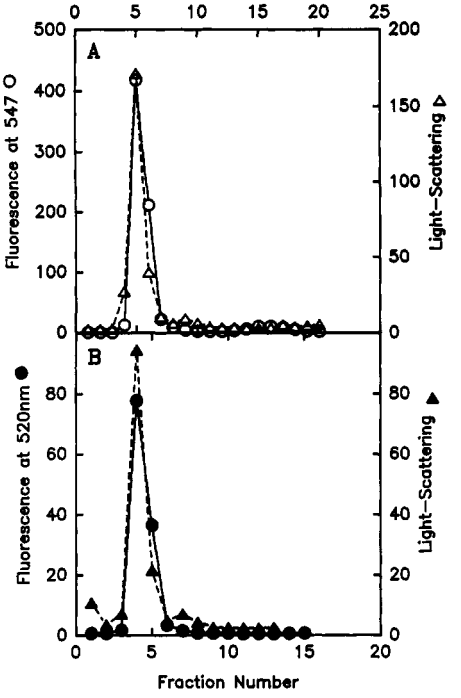

FIGURE 3: Sepharose 6B column chromatography of 7:1 DPPC–DPPG vesicles containing native SP-C, NBD-SP-C, and EITC-SP-C. (A) (○) Fluorescence at 547 nm of vesicles containing EITC-SP-C and (△) light scattering at 360 nm of vesicles containing native SP-C. (B) (●) Fluorescence at 520 nm of vesicles containing NBD-SP-C and (▲) light scattering at 360 nm of vesicles containing native SP-C.

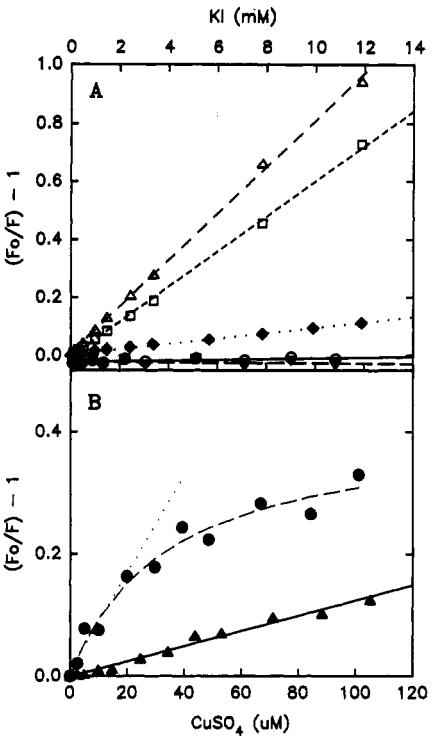

FIGURE 4: Stern–Volmer plot of collisional quenching of NBD-SP-C and EITC-SP-C fluorescence. The straight lines represent the best fit straight lines to the data. (A) Quenching of NBD-SP-C fluorescence by KI, compared with NBD-labeled lipid probes. Excitation was at 460 nm and emission at 520 nm. Aqueous KI quenching experiments were conducted in MNE buffer containing 20 mM $Na_2S_2O_3$. Symbols: (△) NBD-SP-C in methanol, (□) NBD-hexanoic acid in methanol, (◆) NBD-Leu in MNE buffer, (○) NBD-SP-C in 7:1 DPPC–DPPG vesicles, and (▼) NBD-PC in 7:1 DPPC–DPPG vesicles. (B) Quenching of EITC-SP-C fluorescence by $CuSO_4$, compared with EITC-leucine, in 120 mM NaCl and 10 mM MOPS, pH 7.0. Excitation was at 520 nm and emission at 547 nm. Symbols: (●) EITC-SP-C in 7:1 DPPC–DPPG vesicles [the dashed line is the best fit to the data calculated according to Gelborn and Sawyer (1978), eq 10; the dotted line represents the initial slope at low Cu^{2+} concentration); (▲) EITC-leucine in buffer.

fluorescence maximum of NBD-SP-C in methanol is 526 nm and in chloroform, 517 nm. NBD-labeled leucine (NBD-Leu), a water-soluble analogue of NBD-SP-C, had a fluorescence emission maximum of 540 nm in MNE buffer. In 7:1 DPPC–DPPG vesicles, the emission maximum of NBD-SP-C is 525 nm, similar to NBD-PC, reflecting a moderately hydrophobic environment (Chattopadhyay & London, 1988).

The accessibility of the fluorescent moiety of NBD-SP-C was monitored by collisional quenching with KI in both methanol and DPPC–DPPG vesicles, which were sonicated to produce unilamellar vesicles for this experiment. Quenching of NBD-SP-C was compared with that of NBD-hexanoic acid (NBD-HA) in methanol, with NBD-Leu in buffer, and with NBD-PC in vesicles (Figure 4A). When the quenching was plotted according to the Stern–Volmer equation, a straight line was obtained, consistent with a collisional mechanism. The slope of the quenching plots is equal to the quenching constant $k_q\tau$, where k_q is the quenching rate constant and τ is the lifetime of the dye in the absence of quencher. The small slope observed for NBD-SP-C in vesicles, 1.4 M^{-1}, as compared to the slope observed in methanol, 80 M^{-1}, indicates that the NBD moiety of NBD-SP-C is strongly protected from collisional quenching by the aqueous quencher KI when incorporated in vesicles. For comparison, the slope observed for NBD-Leu in buffer, which should be accessible to quenching by KI, is 9.2 M^{-1}. The lipophilic probe NBD-PC is inaccessible to quencher when incorporated into vesicles (slope = –0.8 M^{-1}). Both the quenching results and the location of the fluorescence maximum of NBD-SP-C strongly suggest that the NBD moiety is buried within the membrane bilayer.

For EITC-SP-C, the degree of quenching with KI in methanol was low, so an alternative quenching agent, $CuSO_4$, was used. $CuSO_4$ quenched EITC-SP-C strongly in methanol, but in a nonlinear manner, probably reflecting ionic binding between Cu^{2+} and the carboxyl group of the eosin in methanol. EITC-labeled leucine, (EITC-Leu) was used as a water-soluble analogue for EITC-SP-C. Quenching of EITC-Leu in MNE buffer was linear, with a quenching constant of 1.25×10^3 M^{-1} at 22 °C (Figure 4B). The fluorescence lifetime of eosin is typically about 1 ns (Porter et al., 1974), giving a k_q estimated from the slope of 1×10^{12} M^{-1} s^{-1}, which is too high to be consistent with a diffusion-controlled process. Thus, binding of Cu^{2+} by EITC-Leu may cause the large degree of quenching observed, in which case the slope represents the association constant. Quenching of EITC-SP-C is sonicated 7:1 DPPC–DPPG vesicles was nonlinear. The downward curvature of the Stern–Volmer plot can result from binding of the Cu^{2+} ion to the vesicle surface (Gelborn & Sawyer, 1978). Although the limiting slope at low concentration, 8030 M^{-1} (dotted line, Figure 4B), exceeds the slope observed with EITC-Leu, this may reflect the larger number of binding sites for Cu^{2+} at the membrane surface as compared to EITC-Leu in solution. Therefore, the location of the EITC moiety relative to the lipid bilayer cannot be determined from these data.

Fluorescence Energy Transfer Results. The fluorescent dyes NBD and eosin provide an excellent overlap for fluorescence energy transfer experiments. The corrected excitation and emission spectra of NBD-SP-C and EITC-SP-C are shown in Figure 5. Both fluorophores have considerable overlap between their own excitation and emission

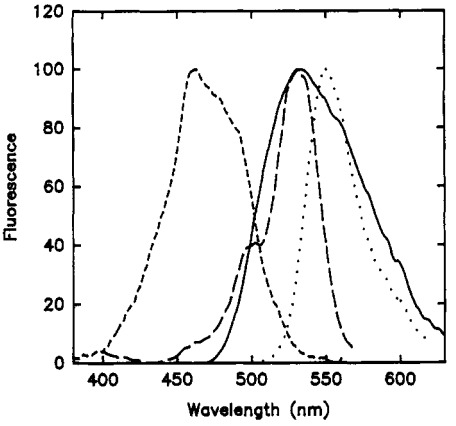

FIGURE 5: Fluorescence excitation and emission spectra of NBD-SP-C and EITC-SP-C in 7:1 DPPC–DPPG vesicles. Curves: (- - -) NBD-SP-C corrected excitation spectrum, emission at 580 nm; (—) NBD-SP-C corrected emission spectrum, excitation at 450 nm; (– –) EITC-SP-C corrected excitation spectrum, emission at 590 nm; (···) EITC corrected emission spectrum, excitation at 480 nm.

Table II: Calculated R_0's for Energy Transfer

temp (°C)	NBD-SP-C to EITC-SP-C R_0 (Å)	EITC-SP-C to EITC-SP-C R_0 (Å)	NBD-SP-C to NBD-SP-C R_0 (Å)
20	66	39	34
37	65	40	33
50	62	41	31

spectra, allowing for considerable self-energy transfer as well. The characteristic energy transfer distances, R_0's, calculated from the spectral characteristics of the dyes are listed in Table II. Note that the R_0 for ET from EITC to EITC is 39 Å, more than half the R_0 for NBD → EITC energy transfer (66 Å). The R_0 for ET from NBD to NBD is also significant, at 34 Å. Although the effect on ET efficiency of interaction among donors is not explicitly treated in our analysis, it is likely to be small. In multiply labeled macromolecules with a donor–donor R_0 equal to one-half the donor–acceptor R_0, the effect of donor–donor interaction is to increase the ET efficiency slightly [by 0.01 for the case of three donors and one acceptor (Gennis & Cantor, 1972)].

For most of the energy transfer experiments a lipid mixture of 7:1 DPPC–DPPG was used to prepare vesicles. This mixture was chosen as having a composition which corresponds to about 80% of the lipid in natural surfactant, while avoiding multiple chain lengths or degrees of saturation which would lead to lipid phase separations. The self-interaction of labeled SP-C was studied by fluorescence energy transfer (ET) as a function of the mole fraction of acceptor-labeled SP-C (EITC-SP-C) and temperature (Figure 6). In order to vary the mole fraction of EITC-SP-C while keeping the surface density of acceptor constant, it was necessary to vary the total SP-C concentration from 1.3% to 6% (w/w, protein:lipid). The increase in surface area due to the addition of SP-C has been neglected but should amount to no more than the maximum percent by weight of SP-C added, that is, 6%. Upon examination of the ET vs temperature curves (Figure 6A), three temperature regions are evident. Above 42 °C, energy transfer is low. The amount of energy transfer observed is approximately equal to the amount expected for a random relative distribution of donor and acceptor in the lipid bilayer, as discussed in more detail below. Between 34 and 42 °C, the amount of ET observed increases dramatically with transition of the lipid environment from the fluid to the gel state. The amount of ET observed below 37 °C is much greater than

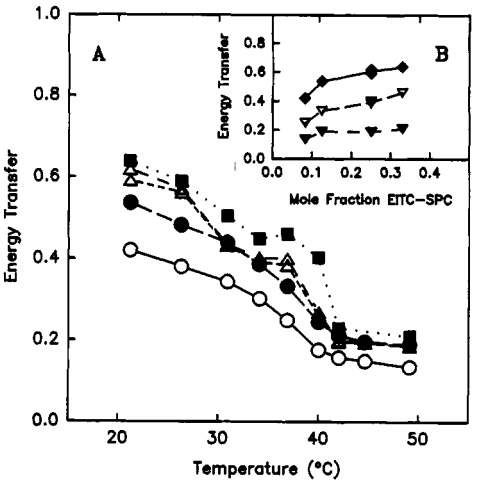

FIGURE 6: Fluorescence energy transfer (ET) from NBD-SP-C to EITC-SP-C in 7:1 DPPC–DPPG vesicles as a function of temperature and mole fraction of EITC-SP-C relative to total SP-C. The surface density of EITC-SP-C was held constant at 9.2×10^{-4} acceptors/phospholipid. The mole fraction of NBD-SP-C relative to total SP-C was held constant at 0.25. (A) ET vs temperature. Mole fractions of EITC-SP-C and total SP-C concentrations (as %, w/w) were (○) 0.083, 6% SP-C; (●) 0.125, 4% SP-C; (△) 0.25, 2% SP-C (two experiments); and (■) 0.39, 1.3% SP-C, (B, inset) ET vs mole fraction of EITC-SP-C at selected temperatures: (▼) 50 °C, (▽) 37 °C, and (◆) 20 °C.

that expected to arise from a random distribution of SP-C in the membrane, indicating self-association of the SP-C monomers. The shape of the ET vs temperature curve is affected by the total concentration of SP-C in the lipid vesicles, reflecting the broadening of the lipid-phase transition produced by SP-C (Horowitz et al., 1992). At 20–25 °C, even greater ET is observed, especially in those samples containing 2% or less total SP-C and a larger mole fraction of acceptor-labeled SP-C. ET at selected temperatures is plotted vs mole fraction of acceptor (EITC-SP-C) in Figure 6B. Above 42 °C ET increases much more gradually with the mole fraction of acceptor than at lower temperatures, demonstrating that the ET observed at lower temperatures arises from a different mechanism than that above 42 °C.

In most of the ET experiments described herein, the vesicles were allowed to cool to room temperature rapidly. In subsequent experiments, some hysteresis in ET measurements was observed in samples containing 2% (w/w) SP-C below 30 °C, depending on the rate at which the sample cooled to 20 °C. When the samples were cooled slowly from 37 °C or above by contact with a circulating water bath, at a rate of approximately 0.3 °C/min, less ET was observed at 20 °C than when cooling had been rapid. The difference was up to 0.1 ET unit, with the final ET at 20 °C equal to or greater than that observed at 30 °C. At temperatures above 30 °C, the ET was not dependent on the rate of cooling. For SP-C concentrations up to 2% (w/w protein:lipid) in samples allowed to cool rapidly to 20 °C, two distinct transitions in ET efficiency occur as the temperature is increased, one between 25 and 34 °C and the other between 37 and 42 °C (Figure 6A). Hysteresis is observed only in the former transition. At higher SP-C concentrations, the transition occurring between 25 and 34 °C is not obvious, and the hysteresis is likewise diminished.

In order to test the hypothesis that the ET observed at temperatures above 42 °C arises from randomly distributed SP-C monomers, a series of experiments were performed in which the surface density of EITC-SP-C was varied but the mole fraction of EITC was kept constant at 0.25 of total SP-C. In Figure 7A, ET is plotted vs surface density of acceptor

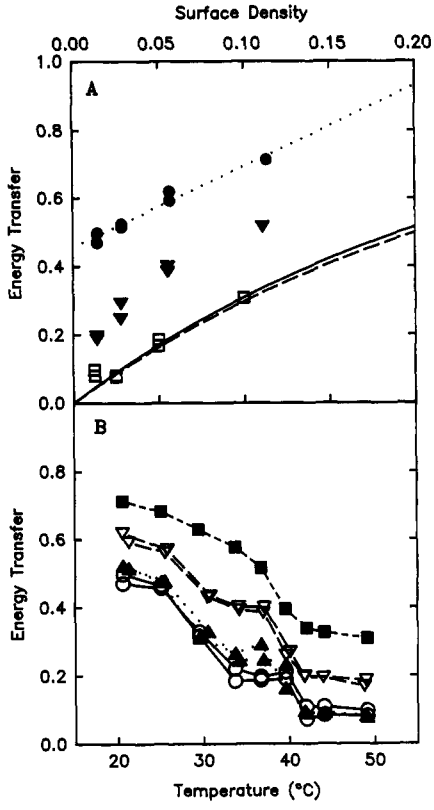

FIGURE 7: ET vs surface density of EITC-SP-C in 7:1 DPPC–DPPG vesicles. The mole fraction of EITC-SP-C was kept constant at 0.25, as was the mole fraction of NBD-SP-C. (A) ET vs surface density of EITC-SP-C. The surface density of EITC-SP-C is expressed as acceptors/R_o^2, at selected temperatures. Temperatures are (●) 20 °C (▼) 37 °C, and (□) 50 °C. The dotted line represents the best fit straight line through the 20 °C data. The curves through the 50 °C data represent ET calculated for R_e/R_o values of (—) 0 and (– –) 0.25, using eq 17 of Wolber and Hudson (1979). (B) ET vs temperature at various surface densities of acceptor. Surface densities of EITC-SP-C (in acceptors/phospholipid) and total SP-C concentrations (in %, w/w, protein:lipid) are (○) 2.3×10^{-4}, 0.5% SP-C; (▲) 4.6×10^{-4}, 1% SP-C; (▽) 9.2×10^{-4}, 2% SP-C; and (■) 1.8×10^{-3}, 4% SP-C. Except for the highest concentration, all experiments were performed in duplicate.

(expressed as acceptors/R_o^2) at three different temperatures, 20, 37, and 50 °C. The ET observed at 50 °C was compared with the energy transfer expected for randomly oriented donors and acceptors in a bilayer, using eq 17 of Wolber and Hudson (1979). For randomly oriented donors and acceptors, ET can be calculated from the number of acceptors/R_o^2 and the ratio of R_e/R_o, where R_e is the distance of closest approach between donor and acceptor. The ET observed at 50 °C in multilamellar vesicles in the experiments presented here can be adequately modeled using the equations for a planar bilayer, where R_e is approximately 0–0.25 times the R_o, or up to 15 Å (Figure 7A, solid and dashed lines). However, the large R_o for ET of the NBD-SP-C and EITC-SP-C pair should allow considerable ET to occur across the bilayer (Dewey & Hammes, 1980; Wolf et al., 1992) and perhaps, in multilamellar vesicles, from one lamella to the next. If trans-bilayer ET contributes significantly to the observed ET, the actual R_e would have to be larger than 15 Å to give an ET as low as that observed. Nevertheless, it is clear that the data obtained at 42–50 °C are well within the range of ET expected among randomly oriented, noninteracting donors and acceptors, leading to the conclusion that SP-C is primarily not self-associated in DPPC–DPPG vesicles above 42 °C.

The data are plotted as ET versus temperature in Figure 7B. A sharp transition in ET efficiency occurs at the phase

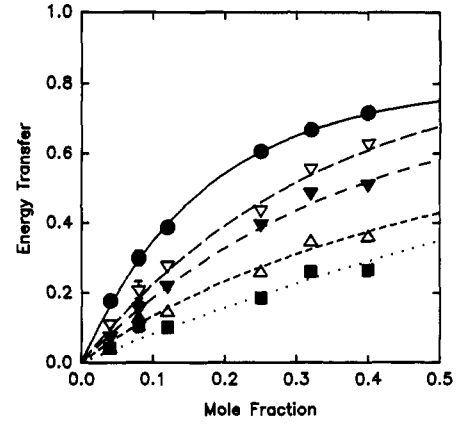

FIGURE 8: Energy transfer from NBD-SP-C to EITC-SP-C versus mole fraction of EITC-SP-C, with total SP-C held constant at 2% (w/w, protein:lipid). Data were taken at the following temperatures: (●) 20 °C, (▽) 30 °C, (▼) 37 °C, (△) 40 °C, and (■) 50 °C. The curves are the best fit to the data using eq 3 (text), with k = 4.35. The parameters f_p and C_p are listed in Table III. The points at 0.08 and 0.25 mole fraction represent the averages of two experiments, for which the variation has been indicated by error bars.

transition temperature of the bulk lipid (between 41 and 42 °C in samples containing 1% or less SP-C). As noted above, the transition becomes broader as the total SP-C concentration increases. Aggregation of SP-C within the membrane could result either from protein–protein interactions giving rise to specific oligomers or from formation of protein-rich patches due to protein–lipid interactions, such as exclusion of SP-C by gel-phase lipids. With regard to the case of oligomerization, a lower limit on the amount of ET arising from oligomers may be obtained by extrapolating the ET results to zero surface density, where the contribution due to noninteracting donor and acceptor must be zero. This approach yields a minimal degree of association, since the degree of oligomerization should decrease as the total SP-C concentration decreases. At 20 °C an ET value of 0.46 was obtained for the y-intercept of the best fit straight line (Figure 7A, dotted line). For a dimer, the maximum possible ET is equal to the mole fraction of acceptor-labeled SP-C present. The y-intercept at 20 °C, 0.46, exceeds the mole fraction of acceptor, 0.25. On the basis of the probability of a donor participating in the same oligomer with an acceptor, which depends on the mole fraction of acceptor present (Veatch & Stryer, 1977), it can be shown that if either trimers or tetramers are the largest oligomer formed, they must account for more than 80% of the SP-C present. At 30 °C, the y-intercept is 0.25, and at 37 °C, it is 0.17. Therefore, at these temperatures, the ET observed could be caused by dimerization only if the ET efficiency within the dimer were close to 1 and the association constant quite favorable.

In a further series of experiments, the total SP-C concentration was kept constant at 2% (w/w) to avoid the effects of varying protein concentration, while the mole fraction and surface density of EITC-SP-C were varied. In Figure 8, ET in vesicles containing 2% SP-C has been plotted against the mole fraction of acceptor at various temperatures. If the large ET observed at low temperatures arises from aggregation or "patching" of SP-C, the ET will depend on the fraction of SP-C which is contained in aggregates and the local surface density of SP-C within the aggregates. Since the ET at 50 °C appears to arise from nonaggregated SP-C, the ET data obtained at 50 °C can be used as a standard curve for the dependence of ET on the concentration of acceptor-labeled SP-C (EITC-SP-C). The extent of aggregation at lower

Table III: Aggregation of SP-C Estimated from Energy Transfer in 7:1 DPPC–DPPG containing 2% SP-C

temp (°C)	f_p	C_p[a] (×10⁵)	C_r[a] (×10⁵)	standard error[b]
20	0.76	32	1.4	0.0084
30	0.86	16	0.9	0.019
37	0.69	16	2.0	0.016
40	0.16	31	4.4	0.020
50				0.024

[a] Concentrations in SP-C molecules per Å². [b] Standard error of the fit to the data using eq 3 with $k = 4.35R_0^{-2}$.

temperatures can then be estimated by comparison with the ET at 50 °C. The dotted line in Figure 8 indicates the best fit of the 50 °C data to the empirical exponential function:

$$E = 1 - e^{-kMFR_0^2[SP\text{-}C]} \quad (2)$$

where MF is the mole fraction of SP-C which is labeled with acceptor and [SP-C] is the total surface concentration of SP-C in the membrane in molecules/Å². In calculating the total surface area of the membrane, 70 Å² was used as the surface area occupied per lipid (Lewis & Engelman, 1983) and 300 Å² as the area occupied by the probable membrane-spanning α-helix of a molecule of SP-C. The value derived from the fit for the constant k was 4.35 R_0^{-2}.

Assuming that SP-C within patches is randomly oriented and noninteracting and that fluorescent labeling does not alter the propensity of SP-C to aggregate or patch, the degree of aggregation of SP-C at various temperatures was estimated from the data in Figure 8. The ET observed will be a linear combination of the ET efficiency of the fraction of SP-C contained in patches (E_p) and the ET efficiency of the SP-C which is randomly oriented in the bulk lipid (E_r):

$$E_{obs} = f_r E_r + f_p E_p = f_r(1 - e^{-kMFR_0^2C_r}) + f_p(1 - e^{-kMFR_0^2C_p}) \quad (3)$$

where f_r is the fraction of SP-C in bulk lipid, f_p is the fraction of SP-C in patches, and $f_p + f_r = 1$. C_r and C_p are the concentrations of SP-C in bulk lipid and in patches, respectively, and are related to the total SP-C present by mass balance.

Equation 3 was fit to the data at selected temperatures to generate the curves shown in Figure 8. Because of the assumptions required for this approach, these numbers must be treated only as estimates. Below 40 °C, the value derived for f_p is 0.7 or greater; that is, more than 70% of SP-C is contained within patches (Table III). The concentration of SP-C required to produce the observed ET would be more than three times the overall concentration (i.e., total SP-C/total lipid, which was 5×10^{-5} molecules/Å²) and at least eight times the concentration of SP-C remaining outside the patches. At 20 °C, the aggregation is still more pronounced. The concentration of SP-C in patches at 20 °C appears to be almost doubled relative to the concentration in patches at 37 °C. In view of the hysteresis observed in ET below 30 °C, the additional aggregation apparent at 20 °C may represent aggregated SP-C which has been "frozen out" of the rapidly cooling lipid, forming patches more enriched for SP-C than is the equilibrium condition. Between 30 and 37 °C, where no hysteresis is observed, the majority of the SP-C present in 7:1 DPPC–DPPG vesicles is contained in aggregates.

Effect of Lipid Composition on SP-C Self-Association. The change from a self-associated state to one in which no self-association is apparent (as observed by NBD-SP-C to EITC-SP-C ET) occurs close to 42 °C, the phase transition

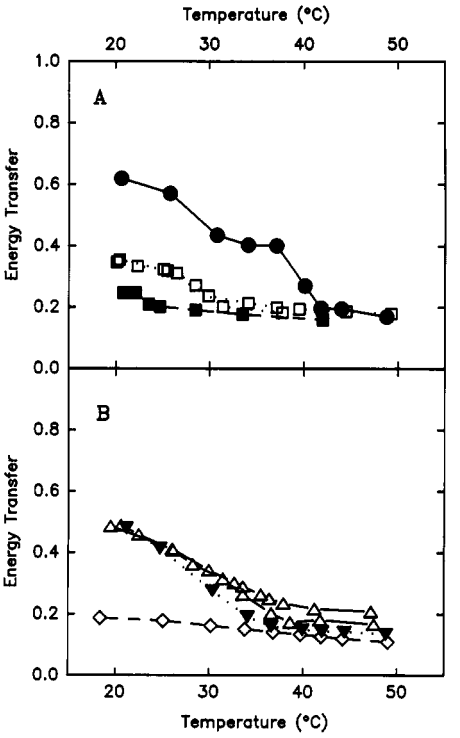

FIGURE 9: Effect of lipid composition on ET from NBD-SP-C to EITC-SP-C. The total SP-C concentration was 2% (w/w, protein: lipid). The mole fractions of NBD-SP-C and EITC-SP-C were 0.25. The lipid mixtures (weight ratios) are (A) (●) 7:1 DPPC–DPPG, (□) 4:3:1 DMPC–DPPC–DPPG (two experiments shown), and (■) 6:1 DMPC–DMPG and (B) (△) 21.6:5.3:3:3.5:1:1:0.87 DPPC–POPC–DPPG–DMPC–DSPC–POPG (EITC-SP-C was the sample which was 32% labeled) (two experiments shown), (▼) 8.75:1.25:1.5:1 DPPC–DPPG–POPC–POPG, and (◇) 3:2 POPC–POPG.

temperature of the bulk lipid. If the self-association of SP-C requires the presence of gel-phase lipids or if it is a passive result of the lipid phase transition, it should depend critically on the lipid composition of the vesicles. Therefore, NBD-SP-C to EITC-SP-C ET was studied in vesicles containing DMPC and DMPG, or POPC and POPG. In 3:2 POPC–POPG, which remains in the liquid phase at 20 °C (Marsh, 1990), only ET due to randomly oriented SP-C monomers was observed (Figure 9B). In a mixture of 8.75:1.25:1.5:1 DPPC–DPPG–POPC–POPG, gradual self-association of SP-C was observed to occur below 34 °C. Similarly, in 4:3:1 DMPC–DPPC–DPPG, self-association of SP-C occurs between 30 and 25 °C (Figure 9A). In 6:1 DMPC–DMPG, SP-C self-association occurs between 22 and 23.4 °C, at the phase transition of the lipid (Marsh, 1990). The degree of self-association achieved below the phase transition, as demonstrated by ET, is much lower in 6:1 DMPC–DMPG than in 7:1 DPPC–DPPG, suggesting that the self-association of SP-C may also be dependent on lipid acyl chain length.

To examine the probable state of SP-C in surfactant-like admixtures, NBD-SP-C to EITC-SP-C ET was examined in a lipid mixture resembling that of the natural surfactant. The mixture consisted of 64.8% DPPC, 16% POPC, 10.6% DPPG, 3% DMPC, 3% DSPC, and 2.6% POPG by weight (open triangles, Figure 9B). The total SP-C concentration was maintained at 2% (w/w) with respect to total lipid. The mole fraction of each of NBD-SP-C and EITC-SP-C was 0.25 (Figure 9B). A maximum ET efficiency of 0.49 was observed at 20 °C, the lowest temperature investigated. ET decreased gradually as temperature increased, to a baseline of 0.19 (±0.02) at 38 °C. The transition of this lipid mixture to the fluid phase, as monitored by anisotropy of diphenylhexatriene,

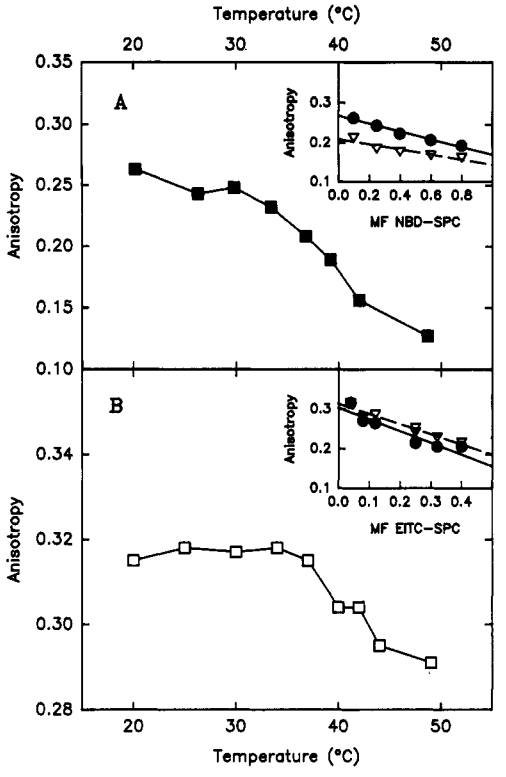

FIGURE 10: Fluorescence anisotropy of NBD-SP-C and EITC-SP-C at a total SP-C concentration of 2%, w/w, in 7:1 DPPC–DPPG vesicles as a function of temperature: (A) (■) NBD-SP-C at a mole fraction of 0.10; (B) (□) EITC-SP-C at a mole fraction of 0.04. Insets: Depolarization of (A) NBD-SP-C and (B) EITC-SP-C fluorescence as a function of the mole fraction of fluorescently labeled probe in 7:1 DPPC–DPPG vesicles, at selected temperatures. The total SP-C concentration was 2% (w/w, protein:lipid). Temperatures for both panels are (●) 20 °C and (▽) 37 °C.

is essentially complete at this temperature (data not shown). Above 38 °C ET remained constant. Thus at 37 °C in this lipid mixture, SP-C is primarily not in a self-associated state.

Anisotropy of NBD-SP-C and EITC-SP-C. Fluorescence anisotropy provides information about the mobility of the labeled molecule. The anisotropies of NBD-SP-C and EITC-SP-C were monitored in lipid vesicles as a function of temperature and mole fraction of labeled SP-C (Figure 10). The anisotropy vs temperature curves shown in Figure 10 represent the lowest mole fraction of labeled SP-C used, with a total SP-C concentration of 2% (w/w protein:lipid). Both fluorescent SP-C samples have a high anisotropy at 20 °C in DPPC–DPPG vesicles: 0.266 for NBD-SP-C and 0.315 for EITC-SP-C. The anisotropy of NBD-SP-C decreases sharply above 34 °C, in parallel with the phase transition of the DPPC–DPPG mixture in the presence of 2% SP-C (Horowitz et al., 1992).

From the R_0 values listed in Table II, it is evident that both EITC-SP-C and NBD-SP-C have significant R_0's for self-energy transfer. This would lead to a depolarization of EITC-SP-C or NBD-SP-C fluorescence when SP-C is self-associated (Snyder & Freire, 1982; Munkonge et al., 1988). Keeping total SP-C constant at 2% w/w, the anisotropies of NBD-SP-C and EITC-SP-C were measured as a function of the mole fraction of protein which was labeled. In these experiments, surface density of the fluorophore increases concomitantly with the mole fraction of labeled protein. In both cases, anisotropy decreased as the mole fraction of labeled SP-C increased, at the same temperatures where self-association was detected in the ET experiments (insets, Figure 10). Thus both the anisotropy and the ET experiments demonstrate aggregation of SP-C at low temperatures in 7:1 DPPC–DPPG vesicles.

DISCUSSION

The surfactant protein SP-C has been labeled with the fluorescent dyes NBD-succinimide and eosin isothiocyanate on the amino terminus of the protein. FTIR data indicate that the labeled SP-C samples retained a majority of their native secondary structure (Table I). FTIR spectra of SP-C, NBD-SP-C, and EITC-SP-C were nearly superimposable in the region of 1700–1500 cm^{-1} (Figure 2). In both cases, a small decrease in the proportion of α-helical content was observed in the labeled SP-C as compared with native SP-C. In all forms of SP-C examined, the amount of α-helical structure was within the range which has been reported for native SP-C preparations in lipid films (Pastrana et al., 1991; Vandenbussche et al., 1992; Baatz et al., 1992). The high degree of α-helical content observed in these samples is characteristic of the monomeric form of SP-C, whereas the dimeric form of SP-C has a low α-helical content and high content of β-structures (Baatz et al., 1992).

Wilhelmy surface balance data indicate that NBD-SP-C retained most of the surface tension lowering properties of native SP-C, while the ability of EITC-SP-C to reduce the surface tension of a lipid film was decreased. Reduction of surface tension at the air–liquid interface is the activity of SP-C which has been the most intensively studied *in vitro*; however, the relation of surface activity in a monolayer to the activity of SP-C in vesicles is not clear. The presence of the bulky eosin moiety on EITC-SP-C may reduce its surface-active properties without affecting the aggregation state of the protein. Both NBD-SP-C and EITC-SP-C undergo aggregation when observed individually in 7:1 DPPC–DPPG, as monitored by the depolarization of fluorescence, indicating that the aggregation is not likely to be an artifact of EITC-SP-C. Both NBD-SP-C and EITC-SP-C retained a strong affinity for lipid vesicles when chromatographed on Sepharose 6B.

Collisional quenching of NBD-SP-C in lipid vesicles by the aqueous quencher KI indicates that the NBD moiety must be buried in the nonpolar region of the bilayer. Therefore, the amino terminus of SP-C must penetrate into the bilayer or rest very close to the bilayer surface. The amino-terminal sequence of bovine SP-C is Leu-Ile-Pro-Cys-Cys- (Olafson et al., 1987), where the two cysteines are palmitoylated (Curstedt et al., 1990). The palmitic acyl chains are likely to interact with the hydrophobic region of the bilayer, anchoring the N-terminus close to the bilayer surface. The NBD-SP-C quenching results are in agreement with this structural prediction for SP-C. The location of the EITC moiety relative to the lipid bilayer is less clear and may be affected by the charge on the eosin probe.

Both NBD-SP-C and EITC-SP-C display high fluorescence anisotropies at 20 °C in 7:1 DPPC–DPPG, when the mole fraction of label is kept low, indicating that SP-C molecules, and, in particular, the amino-terminal region of SP-C, are not free to move rapidly on the fluorescence time scale. Mobility increases with temperature, with NBD-SP-C showing the greatest change between 38 and 42 °C, corresponding to the phase transition of the lipid. Since the NBD moiety is attached to SP-C by a hexanoic acid spacer and is buried within the membrane, its anisotropy may reflect the state of the lipid bilayer in the immediate vicinity of SP-C. The eosin probe, on the other hand, is not attached by a spacer and is more likely to directly reflect the state of the amino-terminal region

of SP-C. The anisotropy of EITC-SP-C also decreases with increasing temperature, signifying an increased mobility of the amino terminus of SP-C, although the decrease in anisotropy is much smaller than for NBD-SP-C.

Direct measurement of energy transfer between SP-C molecules was carried out using vesicles containing NBD-SP-C as a donor and EITC-SP-C as an acceptor. Above 42 °C in 7:1 DPPC–DPPG vesicles, the amount of ET observed was consistent with little or no self-association of SP-C monomers. The large increases in ET observed at temperatures below 42 °C, even after the changes in R_0 and mobility are taken into account, must arise from association of the labeled proteins. From these data, we cannot definitively distinguish between the formation of specific oligomers of SP-C and the formation of aggregates or patches of SP-C. Should SP-C form specific oligomers, they are likely to be greater than dimers at 30 °C, and must be greater than dimers at 20 °C, in order to account for the observed energy transfer. If either trimers or tetramers are the largest oligomer formed, they must account for more than 80% of the SP-C present. Should SP-C form aggregates within the membrane, more than 70% of SP-C must participate in the aggregates. Hysteresis in the ET measurements below 30 °C has been observed and depends on the rate of cooling of the samples. Thus, the additional aggregation observed at 20–25 °C may not be the equilibrium state for SP-C. A possible cause of the hysteresis is the lipid pretransition which occurs around this temperature for DPPC and which has been observed to exhibit hysteresis based on cooling rate (Lewis et al., 1987). The greater lipid ordering expected in the $I_{\beta'}$ phase might result in further exclusion of SP-C into protein-rich patches. Further support for this explanation is provided by the fact that the hysteresis decreases at higher SP-C concentrations, where SP-C is likely to cause more extensive disruption of lipid structure.

Further indications on the nature of SP-C self-association can be obtained by comparison with vesicles of varying lipid composition (Figure 10). It is apparent that the degree of SP-C self-association is high in the presence of gel-phase lipids and low when all lipids are in the fluid phase. Thus, the formation of multimers or aggregates by SP-C either requires the presence of gel-phase lipids or is caused by exclusion of SP-C from gel-phase lipid domains. Aggregation and patching of the intrinsic membrane proteins (Ca^{2+}–Mg^{2+})-ATPase (Munkonge et al., 1988), bacteriorhodopsin (Hasselbacher et al., 1984), and bovine rhodopsin (Borochev-Neori & Montal, 1983) have been observed to occur below the phase transition of the lipid medium at lipid:protein ratios similar to those used in the present experiments. Since SP-C lowers the phase transition temperature of DMPC vesicles (Simatos et al., 1990) and disrupts the acyl chain packing of DPPC/DPPG vesicles sufficiently to allow relief of self-quenching by the lipid probe 6-NBD-PC at low probe concentrations (Horowitz et al., 1992), it is likely that SP-C has a preference for disrupted or fluidlike over gel-phase lipids, suggesting that the aggregation of SP-C occurs by exclusion from the gel phase. However, specific SP-C/SP-C interactions within the aggregates are possible, particularly in view of the high local concentrations of SP-C which are predicted. In a lipid mixture with an acyl chain composition mimicking pulmonary surfactant, ET results indicate self-association of SP-C below 38 °C but no self-association apparent above 38 °C. These experiments were conducted in the absence of Ca^{2+} and surfactant protein SP-B, both of which may affect the arrangement of SP-C in the membrane. Investigation of the effects of SP-B, Ca^{2+}, and the lipid head-group class on SP-C aggregation may help define the roles of each of the elements in surfactant function.

The ET results reported here depend on the behavior of the labeled SP-C molecules reflecting that of unlabeled SP-C. As in any experiment requiring modification of the molecules involved, possible perturbations arising from the modification are an important concern. Ultimately, the elucidation of intermolecular interactions will require comparison of results obtained with a variety of techniques.

The results of the present study lead to a model of SP-C behavior in pulmonary surfactant, in which SP-C may form domains or aggregates in the presence of gel-phase lipids. Although these data do not address the degree of aggregation of SP-C in a lipid film, the demonstrated ability of SP-C to aggregate may apply to the dynamic situation in the lung, in which pulmonary surfactant is subject to pressure changes and possible interconversion between monolayer and bilayer forms during inhalation and exhalation. Within the SP-C domains, lipid structure is likely to be disrupted. The increased rate of spreading of surfactant films brought about by the incorporation of surfactant proteins SP-C and SP-B may also require an increased rate of vesicle fusion with the surfactant monolayer. An increase in fusion and leakiness of lipid vesicles caused by SP-C and SP-B mixtures has been reported (Shiffer et al., 1988). In the present model, SP-C may contribute to the increased rate of vesicle fusion and surfactant spreading in pulmonary surfactant through domains or aggregates in which the lipid structure is disrupted.

ACKNOWLEDGMENT

The authors thank Dr. Darryl Absolom and Ms. Connie Baxter of Abbott Laboratories, Ross Division, for performing the Wilhelmy surface balance measurements, Ms. Ranee Mehra for excellent technical assistance, and Dr. Richard Sleight for critically reviewing the manuscript.

REFERENCES

Baatz, J. E., Elledge, B., & Whitsett, J. A. (1990) *Biochemistry 29*, 6714–6720.

Baatz, J. E., Sarin, V., Absolom, D. R., Baxter, C., & Whitsett, J. A. (1991) *Chem. Phys. Lipids 60*, 163–178.

Baatz, J. E., Smyth, K. L., Whitsett, J. A., Baxter, C., & Absolom, D. (1992) *Chem. Phys. Lipids 63*, 91–104.

Borochev-Neori, H., Fortes, P. A. G., & Montal, M. (1983) *Biochemistry 22*, 206–213.

Cantor, C. R., & Schimmel, P. R. (1980) *Biophysical Chemistry. Part II. Techniques for the Study of Biological Structure and Function*, pp 448–454, W. H. Freeman & Co., San Francisco, CA.

Chattopadhyay, A., & London, E. (1988) *Biochim. Biophys. Acta 938*, 24–34.

Curstedt, T., Jornvall, H., Robertson, B., Bergman, T., & Berggren, P. (1987) *Eur. J. Biochem. 168*, 255–262.

Curstedt, T., Johansson, J., Persson, P., Eklund, A., Robertson, B., Lowenadler, B., & Jörnvall, H. (1990) *Proc. Natl. Acad. Sci. U.S.A. 87*, 2985–2989.

Dewey, T. G., & Hammes, G. G. (1980) *Biophys. J. 32*, 1023–1035.

Fairclough, R. H., & Cantor, C. R. (1978) *Methods Enzymol. 48* (F), 347–379.

Fung, B. K.-K., & Stryer, L. (1978) *Biochemistry 17*, 5241–5248.

Gelborn, K., & Sawyer, W. H. (1978) *Biochim. Biophys. Acta 511*, 125–140.

Gennis, R. B., & Cantor, C. R. (1972) *Biochemistry 11*, 2509–2517.

Goerke, J. (1974) *Biochim. Biophys. Acta 344*, 241–261.

Haas, E., Katchalski-Katzir, E., & Steinberg, I. Z. (1978) *Biochemistry 17*, 5064–5070.
Harwood, J. L., & Richards, R. J. (1985) *Biochem. Soc. Trans. 13*, 1079–1081.
Hasselbacher, C. A., Street, T. L., & Dewey, T. G. (1984) *Biochemistry 23*, 6445–6952.
Hawgood, S., Benson, B. J., Schilling, J., Damm, D., Clements, J. A., & White, R. T. (1987) *Proc. Natl. Acad. Sci. U.S.A. 84*, 66–70.
Horowitz, A. D., Elledge, B., Whitsett, J. A., & Baatz, J. E. (1992) *Biochim. Biophys. Acta 1107*, 44–54.
Johansson, J., Jornvall, H., Eklund, A., Christensen, N., Robertson, B., & Curstedt, T. (1988) *FEBS Lett. 232*, 61–64.
Laemmli, U. K. (1970) *Nature 227*, 680–685.
Lewis, B. A., & Engelman, D. M. (1983) *J. Mol. Biol. 166*, 211–217.
Lewis, R. N. A. H., Mak, N., & McElhaney, R. N. (1987) *Biochemistry 26*, 6118–6126.
Marsh, D. (1990) in *Handbook of Lipid Bilayers*, CRC Press, Boca Raton, FL.
Munkonge, F., Michaelangeli, F., Rooney, E. K., East, J. M., & Lee, A. G. (1988) *Biochemistry 27*, 6800–6805.
Notter, R. H., Finkelstein, J. N., & Taubold, R. D. (1983) *Chem. Phys. Lipids 33*, 67–80.
Notter, R. H., Shapiro, D. L., Ohning, B., & Whitsett, J. A. (1987) *Chem. Phys. Lipids 44*, 1–17.
Olafson, R. W., Rink, U., Kielland, S., Yu, S.-H., Chung, J., Harding, P. G. R., & Possmayer, F. (1987) *Biochem. Biophys. Res. Commun.*, 1406–1411.
Pastrana, B., Mautone, A. J., & Mendelsohn, R. (1991) *Biochemistry 30*, 10058–10064.
Porter, G., Reid, E. S., & Tredwell, C. J. (1974) *Chem. Phys. Lett. 29*, 469–472.
Rice, W. R., Sarin, V. K., Fox, J. L., Baatz, J., Wert, S., & Whitsett, J. A. (1989) *Biochim. Biophys. Acta 1006* (2), 237–245.
Ross, G. F., Notter, R. H., Meuth, J., & Whitsett, J. A. (1986) *J. Biol. Chem. 261*, 14283–14291.
Shiffer, K., Hawgood, S., Düzgünes, N., & Goerke, J. (1988) *Biochemistry 27*, 2689–2695.
Simatos, G. A., Forward, K. B., Morrow, M. R., & Keough, K. M. W. (1990) *Biochemistry 29*, 5807–5814.
Snyder, B., & Freire, E. (1982) *Biophys. J. 40*, 137–148.
Vandenbussche, G., Clercx, A., Curstedt, T., Johansson, J., Jörnvall, H., & Ruysschaert, J.-M. (1992) *Eur. J. Biochem. 203*, 201–209.
Veatch, W., & Stryer, L. (1977) *J. Mol. Biol. 113*, 89–102.
Weast, R. C. (1973) in *CRC Handbook of Chemistry and Physics*, CRC Press, Cleveland, OH.
Weber, G., & Teale, F. W. J. (1957) *Trans. Faraday Soc. 53*, 646–655.
White, C. E., & Argauer, R. J. (1970) in *Fluorescence Analysis, a Practical Approach*, Marcel Dekker, New York, NY.
Whitsett, J. A., Ohning, B. L., Ross, G., Meuth, J., Weaver, T., Holm, B. A., Shapiro, D. L., & Notter, R. H. (1986) *Pediatr. Res. 20*, 460–467.
Whitsett, J. A., & Baatz, J. E. (1992) in *Pulmonary Surfactant System* (VanGolde, L. M. G., Batenburg, J. J., & Robertson, B., Eds.) pp 55–75, Elsevier Academic Publishing Division, Amsterdam.
Wilkinson, D. G., Bailes, J. A., & McMahon, A. P. (1987) *Cell 50*, 79–88.
Wolber, P. K., & Hudson, B. S. (1979) *Biophys. J. 28*, 197–210.
Wolf, D. E., Winiski, A. P., Ting, A. E., Bocian, K. M., & Pagano, R. E. (1992) *Biochemistry 31*, 2865–2873.
Yu, S. H., & Possmayer, F. (1986) *Biochem. J. 236*, 85–89.